

Cite this: *RSC Sustainability*, 2024, 2, 4028

Beyond waste: cellulose-based biodegradable films from bio waste through a cradle-to-cradle approach

Mai N. Nguyen,^a Minh T. L. Nguyen,^{bc} Marcus Frank^{cd} and Dirk Hollmann^{id*bc}

The basis of circular economy is the use and valorization of renewable raw materials. Especially in developing countries, crop waste such as straw and rice straw have high potential for further utilization. Within this report, we present a holistic strategy including the selective isolation of cellulose *via* simple, environmental benign two-step process. Rice straw was easily dissolved in a non-derivatizing electrolyte solvent such as aqueous solution of tetrabutylphosphonium hydroxide (TBPH) (50 wt%) at room temperature followed by precipitation in water. Quantitative amount of raw cellulose was recovered within a short period of time without heating or cooling enabling a further application of biomass material. The structure and characterization of the raw cellulose were investigated by nuclear magnetic resonance (NMR), Fourier transform infrared spectroscopy (FTIR), X-ray diffraction (XRD) and by scanning (SEM) and transmission electron microscopy (TEM). This method could be an excellent alternative to the current extraction methods such as the KRAFT process. Indeed, the same chemicals as for the isolation can be used to prepare regenerated cellulose film of high purity with the raw cellulose. Due to its sustainability and exceptional biodegradability, these films have a great potential for applications in environment, textile, and separation industry. No modification of the cellulose during the extraction and preparation process occurs thus, these films are no plastics and thus can be used without regulations. In general, a full "circular economy" process is provided: valuable raw materials (cellulose) are recovered selectively from natural resources such as rice straw and further to enable products with high applicability in life (cellulose packaging film). The cradle-to-cradle process is closed by fast biodegradation of the used products.

Received 1st October 2024
Accepted 2nd November 2024

DOI: 10.1039/d4su00613e

rsc.li/rscsus

Sustainable spotlight

As the focus of society increasingly shifts to protecting our environment and creating sustainable lifestyles, the importance of innovative research that addresses these challenges continues to grow. The development of technologies and methods that are not only environmentally friendly but also economically viable is a crucial step towards a more sustainable future. The use and valorization of resources that were previously unused or considered as waste plays a key role in this context. The goal is to transform the conventional boundaries of waste management and materials science from a linear economy to a circular economy. So a holistic approach such as a cradle-to-cradle process is particularly important: from nature to nature, without polluting it. Our research aims to make an important contribution to overcoming one of the most pressing challenges of our time: the efficient and sustainable utilization of agricultural waste. By developing a simple but highly effective method of extracting high-purity cellulose from rice straw – a resource that is widely used but underutilized, especially in agricultural countries such as Vietnam – we are paving the way for a new paradigm of waste recycling that is both ecologically and economically viable. Rapid biodegradability in the soil, but also in water, is particularly relevant in order to minimize or even prevent environmental damage. This research aligns with the United Nations Sustainable Development Goals (SDGs), particularly those focusing on responsible consumption and production (SDG 12), climate action (SDG 13) and life on land (SDG 15). The practical and scalable application of sustainable circular chemistry in the conversion of agricultural waste into valuable raw materials is important for global debate and application. Especially in developing countries, simple processes can create added value. The use of renewable resources allows the support of economic development in agricultural communities and can thus protect our planet for future generations.

Main

The challenge of sustainable re-use of waste products has become increasingly important in the global discussion on sustainability¹ and the circular economy.² It is aligned with the United Nations Sustainable Development Goals (SDGs), in particular the goal of responsible consumption and production,

^aSchool of Chemistry and Life Sciences (SCLS), Hanoi University of Science and Technology, No. 1 Dai Co Viet Street, 10000 Hanoi, Vietnam

^bDepartment of Chemistry, University of Rostock, Albert-Einstein-Straße 3A, 18059 Rostock, Germany. E-mail: dirk.hollmann@uni-rostock.de

^cDepartment Life, Light & Matter, Faculty for Interdisciplinary Research, University of Rostock, Albert-Einstein-Straße 25, 18059 Rostock, Germany

^dMedical Biology and Electron Microscopy Centre, University Medicine Rostock, 18059 Rostock, Germany



thus reduces the environmental impact of conventional waste disposal methods. Implementing the re-use of waste in agricultural countries such as Vietnam could not only reduce pollution, but also stimulate new economic sectors and thus contribute to achieving several SDGs. Rice straw has been recognized as a potential alternative for a sustainable, biodegradable and renewable resource. In Vietnam, rice straw is abundant throughout the year and it has been estimated that approximately 67 million tons are produced annually.³ Its main components are cellulose, hemicellulose and lignin, extractive/volatiles as well as a number of minor inorganic compounds such as silica.⁴ The standard treatment mainly comprises the direct burning of rice straw in the farmland because of the quickest and most economical preparation of the fields for the coming growing season. However, this approach not only wastes biomass but also contributes to environmental pollution, destroy public buildings and limit visibility: total rice residue burning emissions as 2.24 Gg high concentrations of fine-particulate matter PM 2.5, together with 36.54 Gg CO and 567.79 Gg CO₂ for Hanoi Province.^{5,6} In contrast, the utilization of straw as a bioenergy or biomass source remains insufficient.⁷ Thus, managing rice straw is not only a challenge but also an opportunity to utilize the available resource and reduce agriculture's climate footprint in agricultural developing countries such as Vietnam.

Cellulose and its derivatives are intensively used in numerous areas such as textiles, packaging, paper production, environment, filtration, agriculture, and medicine.^{8–13} However, the utilization and development of the great potential of cellulose still attracts the attention of scientists based on plenty of attractive features. In recent years, researchers have focused more on the separation of cellulose from biomass, which enables a wide range application in green chemistry.¹⁴ Recently advances the isolation of cellulose can be achieved by various methods, which have advantages and disadvantages in terms of final composition and structural characteristics. These methods can be divided into three main processes, which are physical, biological and chemical or a combination of these processes.¹⁵ Physical treatment such as steam explosion¹⁶ can be carried out to enhance the surface area and accessibility of the biomass for acid or enzyme degradation.^{17,18} While biological treatment uses bacteria and fungi to decompose lignin which has gained popularity due to its advantages over other methods. A biological method is an environmentally friendly and energy-saving process that ensures a high yield of the desired product without the need for special solvents and chemical reagents.¹⁹ However, biological treatment has some disadvantages such as the process takes a long time and requires careful attention and detailed control of microbial growth conditions. Chemical treatment has become one of the most promising methods to degrade lignin in biomass, which decreases the polymerization and crystallinity structure of cellulose. Thus, removal of lignins will help to increase the available surface area and pore volume of the substrate. Acidic and alkali pretreatments have shown of great promise in biomass solubilization.¹⁶ The use of acid aims at dissolving the hemicellulose, leaving lignin and cellulose as solid, while the addition of alkali, usually NaOH, targets mainly

lignin, leaving mainly cellulose as solid with hemicelluloses.²⁰ Indeed, the well-known Kraft process is used without changes over the past 60–80 years producing millions of tonnes of raw cellulose also called Kraft cellulose. They have several benefits, such as simple equipment, easy handling and low cost. However, they induce the formation of toxic by-products such as furfural and hydroxymethyl furfural, potent inhibitors of microbial fermentation. Further disadvantages of the acidic method are the high toxicity and the strong corrosive effect due to the extremely low pH-value, which requires special materials for the reactor design.²¹ Recently a new method involving a one-pot route to achieve cellulose dissolution *via* derivatization were described.²² Ionic liquid immersed as a potential alternative method such as [Emim][acetate] and recently [Emim][formate] plus glycerol.^{23,24} However, no recycling of the ionic liquid has been demonstrated, the role of silica is often neglected in such studies, and high temperatures are required.^{25,26}

Recently it was reported that aqueous electrolyte solution such as TBPH (30 to 60 wt%) readily dissolves cellulose,²⁷ as well as some woody biomass without heating.²⁸ In our previous research, we investigated further co-solvents to enhance processability. However, some solvents were not applicable and precipitation occurs automatically.²⁹ Further testing indicated no precipitation of hemicellulose and lignin with these solvents.

Therefore, in this study, we propose a simple and fast method to dissolve rice straw followed by easy and selective precipitation of cellulose without special equipment or conditions. With the same electrolyte solution (TBPH 50 wt%), the raw cellulose can be used to fabricate the films by the MDCell (abbreviation for the inventors Mai Ngoc Nguyen and Dirk Hollmann cellulose) process.³⁰ The films were characterized in terms of Fourier transform infrared (FTIR), X-ray diffraction (XRD), solid-state dynamic nuclear polarization-enhanced nuclear magnetic resonance spectroscopy (DNP-NMR). The morphology of the synthesized films was investigated by scanning electron microscopy (SEM) and transmission electron microscopy (TEM). To highlight the possibility of a cradle-to-cradle approach we further focused on the biodegradability in soil.

Results and discussion

Isolation of cellulose from rice straw

The detailed procedure for isolation of cellulose using electrolyte solution is illustrated in Fig. 1.

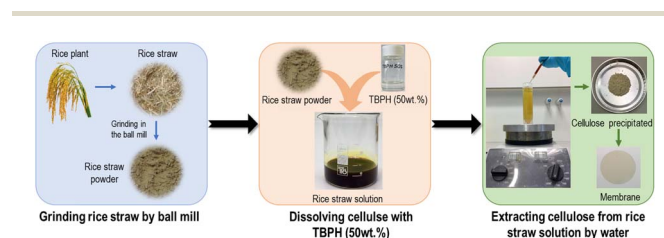


Fig. 1 A schematic diagram of lignocellulosic compound isolation.



First, to increase the accessible surface between rice straw with solvents, rice straw was grinded in a planetary ball mill. Mechanochemistry is considered as a promising method, easy approach and environmentally friendly which can reduce the particle size, increase the contact surface, reduce time for solving, and decrease the degree of crystallinity.^{31,32} In order to produce ultrafine powders, a suitable grinding conditions were obtained by carrying out an evaluation of grinding process. Good distribution and homogeneous powder were found by using pre-cut rice straw (size 0.5 cm in lengths) under grinding conditions: 400 rpm, 180 min in agate material with 15 balls. Then, the finely grinded rice straw was washed in hot distilled water at 60 °C followed by drying at 50 °C in the oven to remove water-soluble extractives such as non-structural sugars and proteins. The dried powder was dissolved in TBPH (50 wt%) at room temperature to get a homogeneous rice straw solution. It has been reported that lignin, hemicellulose as well as cellulose can be dissolved by TBPH (50 wt%).^{27,33,34} To separate the insoluble compounds from the dissolved cellulose, hemicellulose and lignin, the rice straw solution was centrifuged at high speed (14 000 rpm). The residue contained mainly inorganic compound. Note, with the alkaline method such as using sodium hydroxide, the removal of silica was inefficient and affected the purity and quality of cellulose.³⁵ The filtrate was added into a large amount of water resulting in the selectivity precipitation of cellulose as fine fiber (Fig. 2). Water react as an anti-solvent for cellulose solution which weaken and even destroy the hydrogen bonds formed between cellulose and TBPH.²⁹ The precipitated cellulose can be isolated by centrifugation and washing with water. This was proven by a study of the precipitation behavior of dissolved cellulose, hemicellulose and lignin from aqueous TBPH (50 wt%) solution. If these solutions are added to an excess of water, only cellulose was precipitated from the solution. This result can be explained by their structure. In contrast to cellulose, which is made only from glucose, hemicellulose is an amorphous heteropolymer consisting of several different carbohydrates, including xylose, mannose, glucose and galactose in the main chain and arabinose, galactose and 4-*O*-methyl-*D*-glucuronic acid in the side chain. They are water-soluble due to their branched structure.³⁶ Lignin is a three-dimensional amorphous polymer containing ionized phenolic groups making the lignin soluble in a water solution. Lignin precipitation is usually carried out by acidification due to the protonation of the ionized phenolic groups on the lignin molecules.^{37,38}

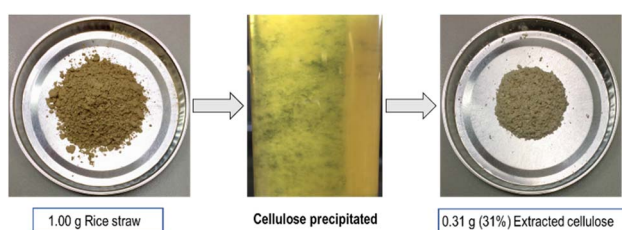


Fig. 2 Isolation of raw cellulose from rice straw.

Thus, with this simple process, cellulose is precipitated easily and selective. Raw cellulose contents 25.9–30.7 wt% of the rice straw were achieved. It corresponds nicely to the theoretical maximum amount of cellulose in rice straw.

Structural characteristics and chemical composition of raw cellulose

To prove the success of the raw cellulose, the rice straw after removing insoluble compounds (Fig. 3a), the raw cellulose (Fig. 3b) and the remaining filtrate (Fig. 3c) were analyzed by the liquid state ¹³C NMR measurement (Fig. 3).

The rice straw solution shows the signal of cellulose, hemicellulose and lignin as expected (Fig. 3a). However, the intensity of C1 lignin is very weak due to the small amount of lignin. After separation, cellulose with distinct characteristic peaks was obtained (Fig. 3b). The remaining filtrate (Fig. 3c) featured only the signals of hemicellulose and lignin at 103.3 ppm, 65.8 ppm and 56.6 ppm, respectively. No cellulose was detected.

As second method, solid state ¹³C-NMR was applied to check the amount of lignin (Fig. 4). However, even with this method only traces of lignin and no hemicellulose were detected in the raw cellulose (Fig. 4A). Therefore, a purity of >95% can be estimated. Notably, the signals from 180 to 120 ppm are attributed to the aromatic carbons of lignin, from 58 to 50 ppm

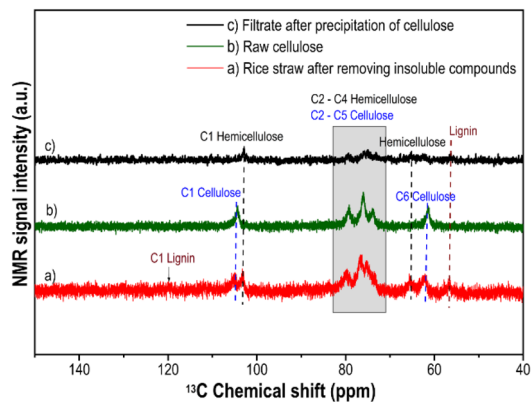


Fig. 3 LS-¹³C NMR spectra of (a) rice straw after removing insoluble compounds, (b) raw cellulose and (c) filtrate after precipitation of cellulose.

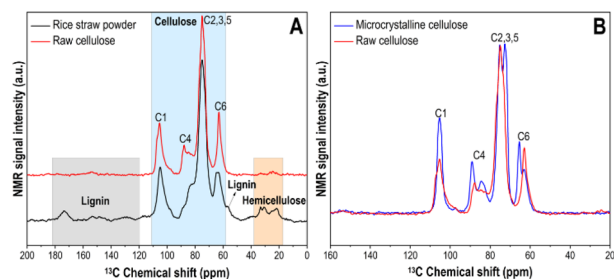


Fig. 4 SS-¹³C NMR (A) between rice straw powder and raw cellulose; (B) between commercially microcrystalline cellulose and raw cellulose.



are related to methoxyl groups ($-O-CH_3$) of lignin^{39,40} and the signal from 30 to 20 ppm are assigned to acetyl groups ($-CO-CH_3$) of hemicellulose.^{40,41} These results indicate the high purity of the precipitated cellulose.

To gain a more comprehensive idea of the structure of raw cellulose, the SS ^{13}C NMR signals of the raw cellulose were compared with commercially available microcrystalline cellulose from cotton linters (Sigma-Aldrich). In Fig. 4B, according to previous studies,^{42–44} the shifts of the C6 but especially the C4 peaks indicating the amorphous structure of the raw cellulose.⁴¹ The changes suggested that hydrogen bonds in crystalline structure of rice straw was disrupted to some extent.

Furthermore, the chemical structure was investigated by FTIR spectroscopy. In rice straw, all major compounds such as cellulose, hemicellulose and lignin are detected (Fig. 5a). The peak at 1728 cm^{-1} (position 1) was assigned to aliphatic esters in lignin and/or hemicellulose in the rice straw.^{45,46} The peak at 1640 cm^{-1} (position 2) can be attributed to the bending mode of the absorbed water and also to carbonyl groups of hemicelluloses.⁴⁷ The peaks at 1512 and 1460 cm^{-1} in the rice straw are indicative of the aromatic $C=C$ stretch in lignin (position 3 and 4).^{48,49} The FTIR spectra of isolated raw cellulose don't show any of these signals indicating again the removal of hemicelluloses and lignin after treatment. Indeed, the FTIR spectra between the isolated raw cellulose (Fig. 5b) and commercially microcrystalline cellulose (Fig. 5c) revealed the similarities. No difference between the spectra were detected. These results suggested that the main component of the precipitated raw material is pure cellulose.

To obtain further information about the macroscopic structure, the XRD patterns (Fig. 5B) of rice straw powder, raw cellulose isolated from rice straw and microcrystalline cellulose

were analyzed. The Rice straw composed of crystalline and amorphous regions.⁵⁰ After grinding rice straw in the ball mill, the rice straw powder's spectrum is broad distribution indicating a large amount of amorphous substances. No distinct polymorphs can be observed. This could be due to the effect of ball mill which change the morphological and structural properties of cellulose.⁵¹

Analyzing the raw cellulose samples revealed the presence of reflections ($2\theta = 12.1^\circ$ (101); 20.1° (102)) which can be assigned to cellulose II. However, the sharper and narrower diffraction peak at (102) clearly demonstrated the increase in the crystallinity of raw cellulose compared with rice straw. During the extraction process, amorphous hemicellulose and lignin were readily dissolved, while leaving the remaining cellulose of a higher degree of crystallinity.⁴⁵ For references as native cellulose, microcrystalline cellulose was analyzed which is composed of cellulose I with three characteristic diffraction peaks ($2\theta = 15^\circ$, 22.4° , and 34.6°).

Utilization as regenerated cellulose films and biodegradability

Recently, we reported a method for fabricating regenerated cellulose films using commercial microcrystalline cellulose.³⁰ This method can now be extended to the utilization of the precipitated raw cellulose. The films consist of 10 wt% raw cellulose in TBPH (50 wt%). Indeed, no difference in chemical composition (detected by FT-IR spectroscopy, Fig. 6A) and the crystallinity (detected by XRD, Fig. 6B) between RC films from raw cellulose or from microcrystalline cellulose (MCC) were observed. In addition, for the membrane application the mechanical durability based on the hydraulic pressure of the flow is important. Indeed, the RC films from raw cellulose collapsed at a pressure of 2.0 bar which corresponds to a maximum flow rate of around 4.0 ml min^{-1} . This was in the range of the cellulose from MCC ($2.5\text{ bar}/4.5\text{ ml min}^{-1}$).³⁰ The film has a smooth and homogeneous surface suggesting a good regeneration of the raw cellulose through the hydrogen-bonding rearrangement of the cellulose macromolecules and fast penetrates of the coagulation reagent propylene carbonate. Noticeable, the film has pale yellow color (Fig. 7A) suggesting a tiny amount of lignin which cannot be detected by the other spectroscopic methods mentioned before.

This forced us to invest the structure and morphology of the films applying Light Microscopy (LM), Transmission Electron Microscopy (TEM), and Scanning Electron Microscopy (SEM). In Fig. 7 a summary of the surface characterization techniques for the most important RC film 1 is shown.

First, the wet RC films were inspected by LM with toluidine blue (Fig. 7B). Here, a homogeneous distribution of the TB over the entire size of regenerated cellulose was detected. The thickness of the wet films decreased to $213\text{ }\mu\text{m}$, which is nearly the same height as for RC film obtained by microcrystalline cellulose ($220\text{ }\mu\text{m}$).³⁰ The reduction in thickness (casting high $500\text{ }\mu\text{m}$) was probably caused by the coagulation process and dehydration during the embedding and resin infiltration process of the membrane for subsequent LM and TEM preparation. Again, no capillary pores were visible. However, small

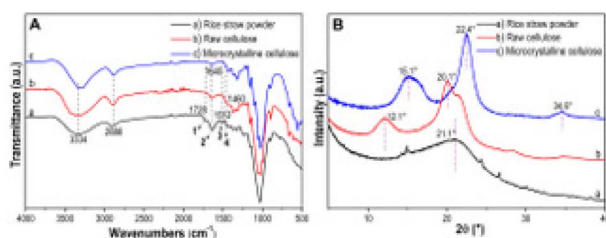


Fig. 5 (A) FTIR spectra and (B) XRD patterns of (a) rice straw powder, (b) raw cellulose and (c) microcrystalline cellulose.

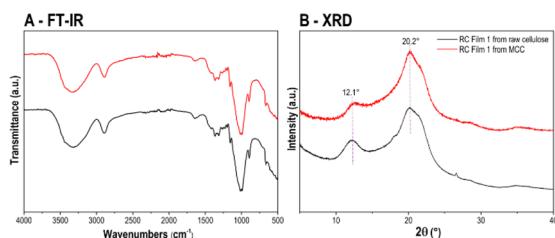


Fig. 6 (A) FT-IR spectra, (B) XRD patterns of the RC films from raw cellulose and microcrystalline cellulose.



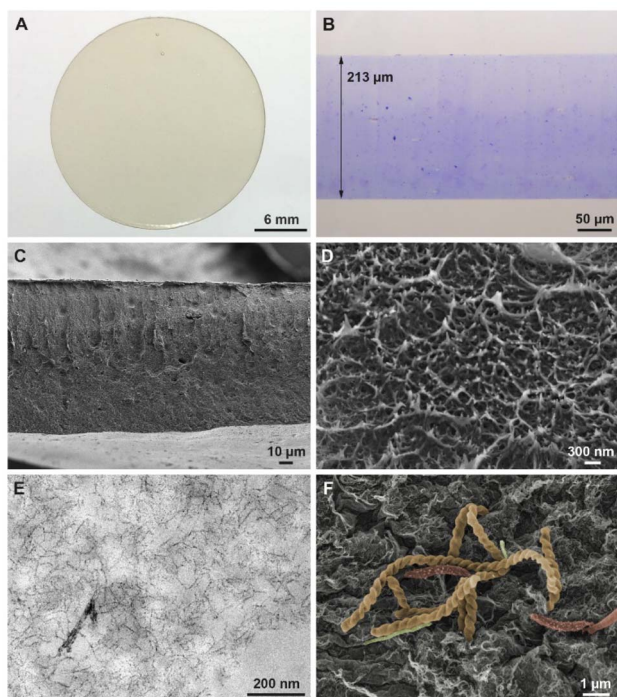


Fig. 7 (A) Picture of the regenerated cellulose films produced from raw cellulose. (B) Light microscopic (LM) image of a semithin cross section of a RC film processed and embedded for electron microscopy section stained with toluidine blue; scale bar is 50 μm . (C) SEM micrograph of a critical point dried membrane which exhibits a compact layering of the RC film structure; scale bar is 10 μm . (D) Higher resolution imaging shows that the film is composed of multiple, densely arranged structured layers of cellulose microfibrils, scale bar is 300 nm. (E) Accordingly, high resolution TEM imaging reveals the ultrastructure of the RC films showing multiple branched cellulose fibrils in a thin section (~ 50 nm) contrasted with lead citrate and uranyl acetate. Note that at places also larger, more densely packed and thus darkly stained structures which are also composed of fibrils are detected; scale bar is 200 nm. (F) SEM image of a membrane surface which was stored in water for more than two months showing bacteria on the surface. The various bacteria were highlighted by layer coloration of the SEM micrograph, scale bar is 1 μm .

more intensely stained particles of unknown origin distributed homogeneously throughout the complete film were observed.

These particles can be detected by SEM (Fig. 7C and D) and more specifically in detail using high resolution TEM imaging as well (Fig. 7E). It seems that still some small undissolved remains of former cellulose fibers or microfibrils are incorporated. Fibrillar composition, *i.e.* the cellulose microfibrils are best visualized with contrast reagents such as lead citrate and uranyl acetate (Fig. 7E). Here, an irregular, net-like structure of branched microfibrils was observed, with a size of the net meshes in the range of ~ 30 – 100 nm. Furthermore, the film surface appears relatively smooth by TEM inspection at the border to the resin. Under SEM conditions (dried in air or critical point dried), an almost perfect surface with a compact, very uniform, dense, but layered structure was detected, with a superior structure preservation in critical point dried samples (Fig. 7C). Again, no capillary pores were observed, however the

film thickness was decreased below 200 μm . The layers and microfibrils observed with high resolution SEM correspond well to the regular distribution cellulose microfibrils seen in TEM. Taken together all microscopic results indicate a fast and homogeneous distribution of the cellulose fibers, similar to earlier observations in films from pure microcrystalline cellulose.

Interestingly after a prolonged time of storage (2–6 months) in (distilled) water we were able to detect multiple bacteria species hosted on and densely attached to the film surface (Fig. 7F). This indicates a descent biodegradability of the membranes even under less favourable conditions in distilled water. Further investigation on the origin and nature of the bacteria are in progress.

This detection was of great importance, as it shows how well the film can degrade even under very low bacterial conditions. Therefore, we were particularly interested in the biodegradability of the film in soil. The test was performed at 20 degrees inside the soil (Fig. 8B, depth 2 cm) and at 20 degrees on the surface (Fig. 8A). For the soil test, the samples were clamped in

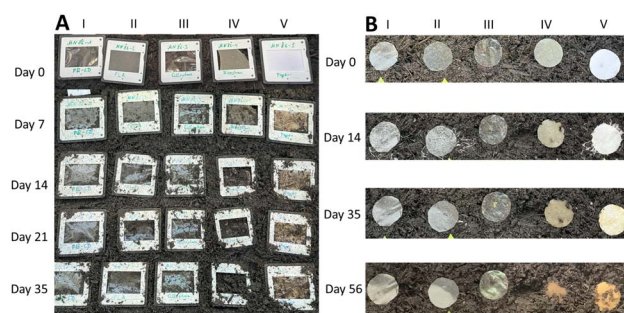


Fig. 8 Biodegradability test of (A) inside the soil (films are fixed in a Dia frame), and (B) on the soil surface. (I) PE foil, (II) PLA foil, (III) Cellophane "Natureflex", (IV) RC film 1, (V) paper.

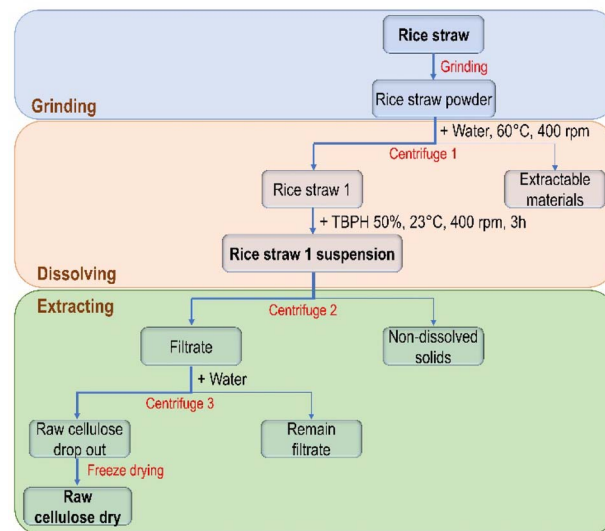


Fig. 9 A detailed procedure for isolation of cellulose using TBPH (50 wt%).



a Dia frame, buried and excavated as well as photographed after 7 days. LDPE film, PLA film, cellophane film and paper were tested for comparison.

Compared to all these films, inside the soil our film degrades completely within 4 weeks. This occurs with no release of microplastics. Which would also be unlikely under these conditions since the film consists only of cellulose. Surprisingly, the Cellophane NatureFlex (Fig. 8A(III) and B(III)), which is currently sold as a sustainable cellulose material, has not degraded a single bit. Note that MCC cellulose materials is also degrading even in water.⁵² On the surface, the degradation takes a longer since bacteria can only attack from one side and decompose the film. Complete decomposition occurs after 2 months. Further water biodegradability test in our laboratory and under real conditions are in progress.

Conclusion

In this study, we presented an easy, simple, and fast strategy to approach selectively high purity cellulose from renewable bio waste such as rice straw. By selectively isolating cellulose from rice straw and converting it into biodegradable films, we offer an innovative solution for upgrading biowaste.

The cellulose obtained is nearly free of contaminated lignin and hemicelluloses. No special requirements, heating or conditions are necessary. The chemicals used are non-toxic and aqueous solvents can be used. The dissolution of all rice straw material in TBPH 50 wt% simply followed by precipitation in water enables the recovery of a quantitative amount of cellulose. The same chemicals can be used to utilize the raw cellulose obtained towards to high quality regenerated cellulose films. These films exhibit an excellent biodegradability compared to other known packaging materials. Future investigations and applications are under progress. This is a future-oriented green “Cradle-to-Cradle” alternative to known industrial processes to valorize biomass but especially bio waste. It represents a significant step forward in the development of a circular economy by converting a waste product into a valuable raw material.

Methods

Procedures

The procedure for isolation of cellulose using electrolyte solution is illustrated in Fig. 9 according to the following 3 steps: grinding, dissolving and extraction.

Grinding rice straw by the planetary ball mill. Simple grinding process was carried out in the Planetary Ball Mill Retsch PM 200, which can be done by loading 1 gram dried rice straw 0.5 cm lengths with 15 balls into a rotated milling vial with speed 400 rpm in 180 minutes. Agate material for the ball and the vial was used.

Dissolution of rice straw. 1 gram rice straw powder was mixed into a flask containing 80 ml distilled water at 60 °C for 2 hours to remove all the water-soluble extractives. Following that, the insoluble residue was collected by centrifuging at room temperature at 4000 rpm in 20 minutes. The substrate was then

washed 3–4 times with distilled water, followed by drying at 50 °C overnight, and labeled as rice straw 1. After removing the extractives, rice straw 1 was dissolved in TBPH (50 wt%) at room temperature (23 °C) at 400 rpm for about 3 hours ensuring the complete dissolution.

Precipitation of cellulose in water from rice straw solution.

The solution was separated to filtrate and solids by centrifuge with 14 000 rpm in 20 minutes. The solid was washed 1–2 times with TBPH (50 wt%) and combined with the filtrate. The filtrate was added dropwise into water under vigorous mixing enabling the selective precipitation of cellulose. The raw cellulose was washed many times with pure water, followed by freeze drying.

Film preparation. A typical process for preparing regenerated cellulose films as follows the reported MDCell method 24. Raw cellulose (10 wt%) was dissolved in TBPH (50 wt%) within 60 minutes at room temperature and under stirring 400 rpm. Then, the resulting clear solution was casted with the casting knife (500 μm) onto a glass plate with a speed of 5 mm s⁻¹ to get a cellulose layer. The cellulose layer was immersed into a propylene carbonate bath for coagulation. Finally, the regenerated cellulose films were washed within distilled water to remove all water-soluble chemicals and impurities.

Biodegradability. The biodegradability tests were carried out with standard soil (standard flower soil) purchased from Kaufland. Standard LDPE (low density polyethylene), PLA (polylactic acid), cellophane (Natureflex from Futamura) and standard paper (purchased from HP) were tested for comparison. Rectangular sections of 3.5 × 2.5 cm were cut and positioned in a frame. These film samples were buried in the soil to a depth of 2 cm.

Materials

Rice straw was harvested from a local farm in Thai Binh Province, Vietnam and was cut into small pieces of about 0.5 cm by a crusher. Tetrabutylphosphonium hydroxide (TBPH) containing 40 wt% in water was purchased from Acros and concentrated through rotary evaporation under 70 bar, 40 °C to get a higher concentration (50 wt%). Microcrystalline cellulose (MCC, powder, 20 μm), propylene carbonate (PC, 99.7% purity) and dimethyl sulfoxide (DMSO) were supplied from Sigma-Aldrich.

Characterizations

Fourier transform infrared spectroscopy (FT-IR). Infrared spectra of samples were investigated with a Bruker FT-IR Alpha II spectrometer in ATR mode. The specimens were measured directly with wavenumbers range from 400 cm⁻¹ to 4000 cm⁻¹.

Solid-state nuclear magnetic resonance. Solid-state NMR experiments were performed under magic angle spinning (MAS) using a Bruker AVANCE III HD spectrometer operating at 400.2 MHz proton frequency with a Bruker ASCEND DNP 9.4 T widebore (89 mm) magnet and a MASWVT400W1 BL4 X/Y/H triple channel probe operating in double-resonance mode. Samples were spun in 4 mm ZrO₂ rotors (Bruker) at room temperature and 8 kHz MAS frequency. Radio frequency (rf) pulse powers were set to 83 kHz and 50 kHz for ¹H and ¹³C,



respectively. ^1H power was matched to ^{13}C during Hartmann–Hahn cross polarization (CP) with 1.5 ms contact time, SPINAL64 at 83 kHz was used for broadband decoupling of ^1H during the detection windows of 20 ms with a recycle delay of 1 s. Spectra were processed in TopSpin 4.0.6 (Bruker) by exponential window multiplication (EM) with a 50 Hz broadening parameter (LB) before Fourier transform and phase adjustment. The chemical shift was referenced to TMS (0 ppm) by using an external adamantane standard.

X-ray diffraction (XRD). X-ray diffraction (XRD) analysis was performed by using a Panalytical X'Pert diffractometer equipped with an Xcelerator detector using automatic divergence slits and Cu $K\alpha_1/\alpha_2$ radiation (40 kV, 40 mA; $\lambda = 0.15406$ nm, 0.154443 nm). Cu beta-radiation was excluded using a nickel filter foil. The measurements were performed in 0.0167° steps and 100 s of data collecting time per step. The samples were mounted on silicon zero background holders. The obtained intensities were converted from automatic to fixed divergence slits (0.25°) for further analysis. Peak positions and profiles were fitted with the pseudo-Voigt function using the HighScore Plus software package (Panalytical). Phase identification was done by using the PDF-2 database of the International Center of Diffraction Data (ICDD).

Nuclear magnetic resonance (NMR). The samples were measured without using deuterated solvents. The ^{13}C NMR spectra (^1H broadband decoupled) were recorded with a Bruker spectrometer AVANCE Neo 500 at 125.8 MHz (10 000 accumulations, 2 s pulse delay, at 25 °C).

Scanning electron microscopy (SEM). Specimens were air-dried or processed for critical point drying. For critical point drying smaller pieces of the specimens were cut off with razor blades and were dehydrated in an ascending series of acetone. After transfer to a critical point dryer (Emitech K850, Quorum Technologies, East Sussex, UK) specimens were processed further using carbon dioxide as an intermedium for critical point drying. Dry specimens were mounted on SEM stubs with adhesive carbon tape (Plano, Wetzlar, Germany) and coated with a carbon layer of approximately 10–15 nm (Leica SCD500, Leica Microsystems, Wetzlar Germany). Specimens were viewed in a field-emission SEM (Zeiss Merlin VP compact, Carl Zeiss Microscopy, Oberkochen, Germany) equipped with HE-SE and In-Lens-Duo detectors. Images with a size of 1024×768 pixels were recorded at different steps of magnification. Measurements of distances were performed using the SmartSEM measurement tools (Carl Zeiss Microscopy). For visualization of specific structures, coloration of SEM images was carried out using Adobe Photoshop software (Adobe, Mountain View, CA, USA).

Transmission electron microscopy (TEM). Specimens were cut from wet membranes as above to a size of approx. 1×2 mm for subsequent processing for transmission electron microscopy (TEM). After fixation with an aqueous solution of 1% osmium tetroxide for 1 h and washes in distilled H_2O , dehydration through an ascending acetone series to 100% acetone was followed by infiltration with epoxy resin (Epon 812, Serva, Heidelberg, Germany) starting in a 1 : 1 mixture of acetone and resin o/n, followed by pure resin for 4 h. Specimens were

transferred to rubber molds and the resin was allowed to cure at 60 °C for 2 days. The membranes were exposed from the resin blocks with a trimming tool (Leica EM Trim 2, Leica Microsystems, Wetzlar, Germany). Semithin sections (approx. 0.5 μm) and thin sections (approx. 50–70 nm) were cut on an ultramicrotome (Ultracut S, Reichert, Wien, Austria) with a diamond knife (Diatome, Biel, Switzerland). Semithin sections were stained with an aqueous solution of toluidine blue to visualize specimens for further trimming prior to thin sectioning and ultrastructural inspection. Thin sections were transferred to copper grids and were either examined directly without further contrasting agents or were alternatively contrasted with uranyl acetate and lead citrate. The sections were examined on a Zeiss EM902 electron microscope operated at 80 kV (Carl Zeiss, Oberkochen, Germany). Digital images were acquired with a side-mounted $1 \times 2\text{k}$ FT-CCD Camera (Proscan, Scheuring, Germany) using ITEM camera control and imaging software (Olympus Soft Imaging Solutions, Münster, Germany).

Light microscopy. Semithin sections stained with toluidine blue were examined with a light microscope (Zeiss Axioskop 40, Carl Zeiss, Göttingen, Germany) and digital images were recorded with a camera (Zeiss AxioCam ERc5s) using acquisition software with integrated measurement tools (Zeiss ZEN blue edition).

Data availability

The data set to this publication: Beyond waste: cellulose-based biodegradable films from bio waste through a cradle-to-cradle approach [data set] can be accessed *via* Zenodo <https://doi.org/10.5281/zenodo.13867404>.

Author contributions

M. N. N. conceived and performed the experiments for the isolation of cellulose and the synthesis of cellulose films. M. T. L. N. conceived and performed the biodegradability test of the films. M. F. conceived and performed the SEM, TEM and the LM measurements. D. H. formulated and coordinated the overall research goal. This work was supported by funding acquisition through D. H. The manuscript was written through contributions of all authors. All authors have given approval to the final version of the manuscript.

Conflicts of interest

There are no conflicts to declare.

Acknowledgements

This work has been supported by the RoHan Project funded by the German Academic Exchange Service (DAAD, No. 57315854 and 57560571) and the Federal Ministry for Economic Cooperation and Development (BMZ) inside the framework “SDG Bilateral Graduate School Program”. We acknowledge the expert technical support during EM sample preparation of Karoline Schulz, Ute Schulz and Dr Armin Springer. We thank



Dr Victoria Aladin and Prof. Björn Corzilius for the solid-state NMR measurements. Further we acknowledge Dr Henrik Lund for the XRD measurements.

Notes and references

- H. Kopnina, R. Padfield and J. Mylan, *Sustainable Business*, Tayler and Francis Group, 2023.
- G. Kaur, K. Uisan, K. L. Ong and C. S. K. Lin, *Curr. Opin. Green Sustainable Chem.*, 2018, **9**, 30–39.
- World Rice Production 2019/2020*, United States Department of Agriculture (USDA), 2020.
- W. D. Jong and J. R. V. Ommen, in *Biomass as a Sustainable Energy Source for the Future*, John Wiley & Sons, Inc., Hoboken, New Jersey, United States of America, 2014, ch. 2, pp. 36–68, DOI: [10.1002/9781118916643.ch2](https://doi.org/10.1002/9781118916643.ch2).
- R. Gupta, *SANDEE Working Papers*, 2012, vol. 66.
- K. Lasko, K. P. Vadrevu, V. T. Tran, E. Ellicott, T. T. N. Nguyen, H. Q. Bui and C. Justice, *Environ. Res. Lett.*, 2017, **12**, 085006.
- V. B. Agbor, N. Cicek, R. Sparling, A. Berlin and D. B. Levin, *Biotechnol. Adv.*, 2011, **29**, 675–685.
- K. H. Gardner and J. Blackwell, *Biopolymers*, 1974, **13**, 1975–2001.
- H. Zhu, Z. Fang, C. Preston, Y. Li and L. Hu, *Energy Environ. Sci.*, 2014, **7**, 269–287.
- C. Huang, Y. Gao, Y. Chen, Y. Shen and H.-Y. Yu, *J. Clean. Prod.*, 2024, **451**, 142107.
- S. Wang, A. Lu and L. Zhang, *Prog. Polym. Sci.*, 2016, **53**, 169–206.
- N. Sharma, B. J. Allardyce, R. Rajkhowa and R. Agrawal, *Bioengineered*, 2023, **14**, 2242124.
- M. Yang, Y. Chen, S. Y. H. Abdalkarim, X. Chen and H.-Y. Yu, *Int. J. Biol. Macromol.*, 2024, **276**, 133799.
- F. H. Isikgor and C. R. Becer, *Polym. Chem.*, 2015, **6**, 4497–4559.
- D. Ussiri and R. Lal, *Biofuels*, 2015, **5**, 1–30.
- N. Sharma, B. J. Allardyce, R. Rajkhowa and R. Agrawal, *Sci. Rep.*, 2023, **13**, 16327.
- Y. Sun and J. Cheng, *Bioresour. Technol.*, 2002, **83**, 1–11.
- L. Cadoche and G. D. López, *Biol. Wastes*, 1989, **30**, 153–157.
- A. Hatakka, *FEMS Microbiol. Rev.*, 1994, **13**, 125–135.
- V. S. Chang and M. T. Holtzaple, *Appl. Biochem. Biotechnol.*, 2000, **84**, 5–37.
- W. E. Karr and M. T. Holtzaple, *Biotechnol. Bioeng.*, 1998, **59**, 419–427.
- Y. Chen, C. Huang, Z. Miao, Y. Gao, Y. Dong, K. C. Tam and H.-Y. Yu, *ACS Nano*, 2024, **18**, 8754–8767.
- A. Brandt, J. Gräsvik, J. P. Hallett and T. Welton, *Green Chem.*, 2013, **15**, 550–583.
- J. S. Moulthrop, R. P. Swatloski, G. Moyna and R. D. Rogers, *Chem. Commun.*, 2005, 1557–1559, DOI: [10.1039/B417745B](https://doi.org/10.1039/B417745B).
- S. Zhu, Y. Wu, Q. Chen, Z. Yu, C. Wang, S. Jin, Y. Ding and G. Wu, *Green Chem.*, 2006, **8**, 325–327.
- C. G. Yoo, Y. Pu and A. J. Ragauskas, *Curr. Opin. Green Sustainable Chem.*, 2017, **5**, 5–11.
- M. Abe, Y. Fukaya and H. Ohno, *Chem. Commun.*, 2012, **48**, 1808–1810.
- M. Abe, T. Yamada and H. Ohno, *RSC Adv.*, 2014, **4**, 17136–17140.
- M. N. Nguyen, U. Kragl, D. Michalik, R. Ludwig and D. Hollmann, *ChemSusChem*, 2019, **12**, 3458–3462.
- M. N. Nguyen, U. Kragl, I. Barke, R. Lange, H. Lund, M. Frank, A. Springer, V. Aladin, B. Corzilius and D. Hollmann, *Commun. Chem.*, 2020, **3**, 116.
- C. C. Piras, S. Fernández-Prieto and W. M. De Borggraeve, *Nanoscale Adv.*, 2019, **1**, 937–947.
- D. J. Schell and C. Harwood, *Appl. Biochem. Biotechnol.*, 1994, **45**, 159–168.
- H. Yamada, H. Miyafuji, H. Ohno and T. Yamada, *Bioresources*, 2016, **11**, 839–849.
- U. Hyväkkö, A. W. T. King and I. Kilpeläinen, *Bioresources*, 2014, **9**, 13.
- L. Luduena, D. Fasce, V. A. Alvarez and P. M. Stefani, *Bioresources*, 2011, **6**, 1440–1453.
- G. Brunner, in *Supercritical Fluid Science and Technology*, ed. G. Brunner, Elsevier, 2014, vol. 5, pp. 395–509.
- M. A. Gilarranz, F. Rodriguez, M. Oliet and J. A. Revenga, *Sep. Sci. Technol.*, 1998, **33**, 1359–1377.
- W. Zhu and H. Theliander, *Bioresources*, 2015, **10**, 19.
- Y. Lu, Y.-C. Lu, H.-Q. Hu, F.-J. Xie, X.-Y. Wei and X. Fan, *J. Spectrosc.*, 2017, **2017**, 8951658.
- K. M. Holtman, N. Chen, M. A. Chappell, J. F. Kadla, L. Xu and J. Mao, *J. Agric. Food Chem.*, 2010, **58**, 9882–9892.
- W. Cao, Z. Wang, Q. Zeng and C. Shen, *Appl. Surf. Sci.*, 2016, **389**, 404–410.
- H. Kono, T. Erata and M. Takai, *Macromolecules*, 2003, **36**, 5131–5138.
- H. Yamamoto and F. Horii, *Macromolecules*, 1993, **26**, 1313–1317.
- E. R. Alonso, C. Dupont, L. Heux, D. D. S. Perez, J.-M. Commandré and C. Gourdon, *Energy*, 2016, **97**, 381–390.
- E. Abraham, B. Deepa, L. A. Pothan, M. Jacob, S. Thomas, U. Cvelbar and R. Anandjiwala, *Carbohydr. Polym.*, 2011, **86**, 1468–1475.
- S. Sen, J. D. Martin and D. S. Argyropoulos, *ACS Sustain. Chem. Eng.*, 2013, **1**, 858–870.
- X. Chen, J. Yu, Z. Zhang and C. Lu, *Carbohydr. Polym.*, 2011, **85**, 245–250.
- D. Watkins, M. Nuruddin, M. Hosur, A. Tcherbi-Narteh and S. Jeelani, *J. Mater. Res. Technol.*, 2015, **4**, 26–32.
- F. Xu, J.-X. Sun, R. Sun, P. Fowler and M. S. Baird, *Ind. Crops Prod.*, 2006, **23**, 180–193.
- M. K. M. Haafiz, S. J. Eichhorn, A. Hassan and M. Jawaid, *Carbohydr. Polym.*, 2013, **93**, 628–634.
- M. Ago, T. Endo and K. Okajima, *Polym. J.*, 2007, **39**, 435–441.
- M. Bading, O. Olsson and K. Kümmerer, *Chemosphere*, 2024, **352**, 141298.

